IEEE Access
Multidisciplinary ⋮ Rapid Review ⋮ Open Access Journal

Received November 5, 2019, accepted November 29, 2019, date of publication December 9, 2019,
date of current version December 23, 2019.

Digital Object Identifier 10.1109/ACCESS.2019.2958428

Modified Chip-Evacuation Force Modeling and Chip-Clogging Prediction in Drilling of Cortical Bone

AIRONG ZHANG[1,2], SONG ZHANG[1,2], CUIRONG BIAN[3], AND HUI KONG[3]

[1]Key Laboratory of High Efficiency and Clean Mechanical Manufacture of MOE, School of Mechanical Engineering, Shandong University, Jinan 250061, China
[2]Key National Demonstration Center for Experimental Mechanical Engineering Education, Shandong University, Jinan 250061, China
[3]Department of Prosthodontics, Qilu Hospital of Shandong University, Jinan 250012, China

Corresponding author: Song Zhang (zhangsong@sdu.edu.cn)

This work was supported in part by the Major Research and Development Program of Shandong Province under Grant 2015GGX103043, and in part by the Taishan Scholar Project of Shandong Province under Grant ts201712002.

ABSTRACT Chip clogging is one of the fundamental issues faced by the dentists during the drilling of cortical bone. The chip clogging can lead to significant increase in temperature, thrust force and torque, and can even cause the drill bit to break. In this study, a modified chip-evacuation model to estimate the thrust force was developed for drilling of the cortical bone. First, the modified chip-evacuation force model with two parameters was developed based on the flute geometry. A set of drilling tests was conducted to calibrate the model parameters. Secondly, the parameter models were established as functions of spindle speed and feed, and the coefficients were then determined through nonlinear-regression analysis. The importance of cutting parameters on the model parameters was investigated via analysis of variance. Thirdly, the validity of the force model was analyzed by experimental results. Subsequently, based on the gradient of the chip-evacuation force, the chip-clogging prediction was conducted, and the prediction accuracy was assessed by the validation tests. Finally, the effect of cutting condition on the chip clogging was explored. The modified chip-evacuation force model proved to be an effective tool for predicting the thrust force, and the chip clogging could be estimated accurately with a relative error less than 10%. The spindle speed and the feed both had significant effects on the chip-evacuation force and chip clogging. The modified model could provide a better approach to finding how a pecking cycle can be implemented, and then, it can assist surgeons in selecting cutting conditions.

INDEX TERMS Chip clogging, chip-evacuation force, drilling of cortical bone, twist drill.

NOMENCLATURE

F_z	Chip-evacuation force.
F_z (0)	Initial cutting force.
λ	Ratio between the lateral and axial pressure.
D	Drill diameter.
A_0	Half flute area.
μ_f	Coefficient of friction between the chip and the flute.
μ_w	Coefficient of friction between the chip and the hole wall.
l_f	Effective contact length of the chip element with the flute face.
l_h	Effective contact length of the chip element with the flute heel.
l_w	Effective contact length of the chip element with the hole wall.
θ	Angle between the flute face and the plane formed across the flute.
z	Dimensionless depth.
z'	Hole depth.
P	Pressure intensity along the chip flow direction.
κ, ξ	Parameters of the chip-evacuation force model.
F_{model}	Fitting value of the chip-evacuation force from the force model.
F_{exp}	Processed thrust force from the drilling experiment.
$\alpha_0, \alpha_1, \alpha_2, \alpha_3$	Regression coefficients of κ model from the polynomial regression.
$\alpha'_0, \alpha'_1, \alpha'_2, \alpha'_3$	Regression coefficients of κ model from the logarithmic polynomial regression.

The associate editor coordinating the review of this manuscript and approving it for publication was Ming Luo.

$\beta_0, \beta_1, \beta_2, \beta_3$	Regression coefficients of ξ model.
n	Spindle speed of machine tool.
f	Feed of drilling.
dF_z/dz	Gradient of the chip-evacuation force.
z^*	Critical depth.
dF_z^*/dz	Gradient of the chip-evacuation force at critical depth.
$\lambda_0, \lambda_1, \lambda_2, \lambda_3$	Regression coefficients of gradient model.

I. INTRODUCTION

Among the various operations in orthopedic bone cutting, drilling is widely performed, especially in dentistry for repairing bone fractures, inserting screws, and installing prosthetics [1]. The desired outcome of bone drilling is to obtain the required holes without causing mechanical and thermal damage to the bone and the surrounding tissues. However, due to the low ductility of bone [2], drilling of bone produces discontinuous chips that tend to cluster together as the depth of the hole continues to increase, leading to chip clogging. This phenomenon of chip clogging can lead to an abrupt increase in the thrust force and the torque at some particular depth, which is referred to as the critical depth. As the drilling proceeds, it may cause drill-bit breakage once the torque experienced during the drilling process exceeds its threshold value [3]. Some researches have proved that drilling forces were the main contributor to heat generation [4], which can cause thermal necrosis in the treated area [5]. Moreover, increased forces may promote crack formation and crack propagation [6], [7], and thus, reduce the bone strength, which may lead to implant failure because of poor implant-bone adherence [8]. Because the cutting forces prompt in the development of chip clogging, it is critical to control the drilling forces for successful orthopedic surgery.

At present, the drilling of bone in oral surgery is manually conducted by a surgeon using hand drills [9]. To avoid unnecessary damage caused by chip clogging, step-by-step drilling is usually performed in drilling deep holes [10]. It has been found that periodic drill retraction is a suitable method to improve tool life [11] and reduce the cutting temperature of the drilled area. However, the fact that the sensing of drilling forces by the surgeon is subjective [12] makes it difficult to control the pecking cycles. The thrust force and torque during peck drilling were observed to be lower than those during continuous drilling [13]. However, pecking cycle greatly reduces efficiency and increases the discomfort of the patient during the operation. Therefore, it is significant to determine the proper pecking cycles during process planning for orthopedic surgery. Hence, predicting the chip-evacuation force and the occurrence of chip clogging during drilling of bone is highly significant.

In fact, drilling force depends on many factors, such as, the feed rate of the drill bit, the spindle speed, the geometry of the drill used [14], and the quality of the bone [15]. It has been observed that increased feed rate results in increased thrust force and torque during drilling of bone [16]. Lughmani *et al.* [17] revealed, through experimental and numerical methods, that increased spindle speed produced lower thrust force and torque. However, a higher rotational speed could induce an increase in temperature during bone drilling [18]. Previous studies about the effects of drill-bit geometry on the drilling forces emphasized on drill diameter [19], drill point angle [20] and flute geometry [21]. Among these factors, only the feed and the spindle speed can be controlled by the surgeons. Therefore, these two factors were considered when establishing the chip-evacuation force model in the present study.

Based on the knowledge of drilling metal, previous models developed for the prediction of drilling forces suggested that the interrelationship among thrust force, feed rate, and spindle speed could be described as a power function [1], [22]. To predict the drilling forces experienced during the drilling of bone, Allotta *et al.* [23] adopted a theoretical model that considered drill geometry, feed rate and the shear energy required to cut the material. In another study, an analytic formulation [24] was developed based on the chip removal mechanics of oblique cutting [25]. This model considered not only the cutting lips and the chisel edge, but also the manual effect resulted by the feed change. Later, a comparative study was conducted to estimate the drilling forces for different drill bits by using finite-element (FE) analysis [26], and the FE modeling was validated through *in vitro* drilling experiments. Macavelia *et al.* [27] presented a force model of bone drilling for orthopedic surgery using force balance on a differential chip section. The model describes the chip-evacuation force as a function of flute geometry, cutting condition, and hole depth. In more recent years, several predictive drilling-force models have been developed for accurate haptic rendering [28]. Additionally, a mechanistic model was adopted to estimate the thrust force when drilling human femurs at different regions and directions [29]. This model was demonstrated to be a remarkable predictor of the thrust force, but it was based on computed tomography data from different patients.

The main shortcoming of most models presented in existing literature is that they ignored the effect of chip clogging, and assumed that the drilling force was constant and independent of hole depth. Chip clogging during bone drilling was considered in the study by Macavelia *et al.* [27]. However, the prediction for the formation of chip clogging was not discussed. Moreover, this model was proposed by using an equation derived to estimate the chip-evacuation force of drilling metal [30]. Therefore, there is an increasing demand to improve the accuracy of force and chip-clogging prediction for bone drilling.

To address the lack of quantitative analysis for chip-evacuation force and chip clogging, a modified chip-evacuation force model with two parameters for bone drilling was developed in this study. Based on the modified model,

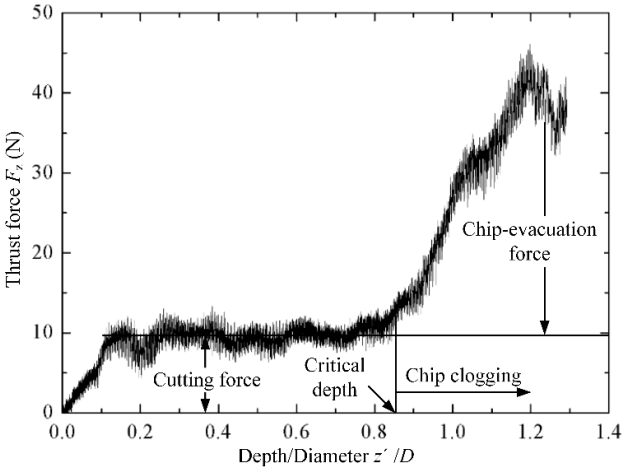

FIGURE 1. Example of thrust force versus depth/diameter at a spindle speed of 600 r/min and a feed of 0.0167 mm/r.

the critical depth of chip clogging was predicted, and thus, the appropriate cutting condition could be determined. First, the modified chip-evacuation force model was established as a function of hole depth, and a calibration procedure was conducted to identify the undetermined parameters. Secondly, the parameter models were developed through regression analysis, and the validity of the chip-evacuation force model was analyzed via drilling experiments. Thirdly, the critical depth for chip clogging in bone drilling was predicted on the basis of the chip-evacuation force, and the prediction accuracy was measured by the experimental results. Finally, the effects of spindle speed and feed on the critical depth were discussed. The model can be used to find the location where chip clogging may emerge in oral surgery, and thus, it assists surgeons in operation planning.

II. MATERIALS AND METHODS

Unlike the drilling of metal, drilling of bone creates discontinuous chips that significantly increase the thrust force, as shown in Figure 1. From the typical profile of thrust force with respect to depth, a sharp rise in the thrust force can be observed when the contact between the drill bit and the cortical bone begins. Then, the removal of material starts at the main cutting edges and the thrust force increases gradually owing to the penetration of the drill bit into the cortical bone. Once the drill bit is fully engaged, the thrust force fluctuates around a constant value, which is referred to as the cutting force. However, the thrust force continues to increase after the point of the critical depth, which marks the onset of chip clogging. The increased thrust force caused by chip clogging is referred to as the chip-evacuation force.

A. CHIP-EVACUATION FORCE MODEL

1) FUNDAMENTAL MODEL FORMULATION

In this paper, a dental twist drill (DHI 2014SM) of stainless steel with a diameter of 2 mm was used to model the chip-evacuation force. Based on the model derived by Mellinger *et al.* [30], the chip-evacuation force, F_z, can be expressed as (1) by using the force balance (Figure 2a) on a differential chip section in the flute. Figure 2b shows the drill cross section.

$$F_z = F_z(0)\, e^{[\lambda D(\mu_f l_f + \mu_f l_h + \mu_f \mu_w l_w \sin\theta)/A_0]z} \tag{1}$$

The dimensionless depth z is defined as the following rule:

$$z = z'/D, \tag{2}$$

the hole depth z' is given in Figure 2a.

Equation (1) indicates that the chip-evacuation force depends on the coefficients of friction when the same drill is used. The coefficients of friction are affected by many factors, such as material, cutting temperature, chip thickness, and velocity between the contacting surfaces. Usually, these factors depend on the cutting condition, e.g., drill diameter, spindle speed, and feed rate. Therefore, the coefficients of friction are expected to remain constant under the same cutting condition. On this basis, (1) can be modified as:

$$F_z = F_z(0)e^{\xi z}. \tag{3}$$

The calibration procedure for (3) could be simplified due to the use of parameter ξ when compared to that for (1). Notably, the model parameters were obtained through experiments of cutting metal in the study by Mellinger *et al.* [30]. The chip-evacuation force was determined by multiplying (3) by a coefficient of correction κ due to the use of different materials, as shown in (4). The parameters of the force model can be determined through a series of calibration experiments.

$$F_z = \kappa F_z(0)e^{\xi z} \tag{4}$$

2) CALIBRATION PROCEDURE FOR MODEL PARAMETERS

The calibration procedure for (4) is described in Figure 3. First, the cutting parameters of bone drilling were determined according to the actual clinical applications. Secondly, the drilling experiments were conducted and the thrust force signals were simultaneously recorded and stored by the computer. Afterwards, the recorded force was processed as follows: i) the cutting force was subtracted from the filtered force signal and ii) the resultant was divided by the number of drill flutes. After the recorded force was processed, the chip-evacuation force model can be expressed as:

$$F_z = \kappa e^{\xi z}. \tag{5}$$

The parameters of the force model can be obtained through a nonlinear least-squares curve fit, as shown in the following form:

$$\min_{\psi} \sum_{z} \left(F_{\text{model}} - F_{\text{exp}}\right)^2, \tag{6}$$

$$\psi = [\kappa\ \xi], \tag{7}$$

where F_{model} is defined in (5). For a given workpiece material and cutting tool, the parameters of the force model are expected to rely only on the spindle speed and the feed. Therefore, as a last step, the polynomial model and the

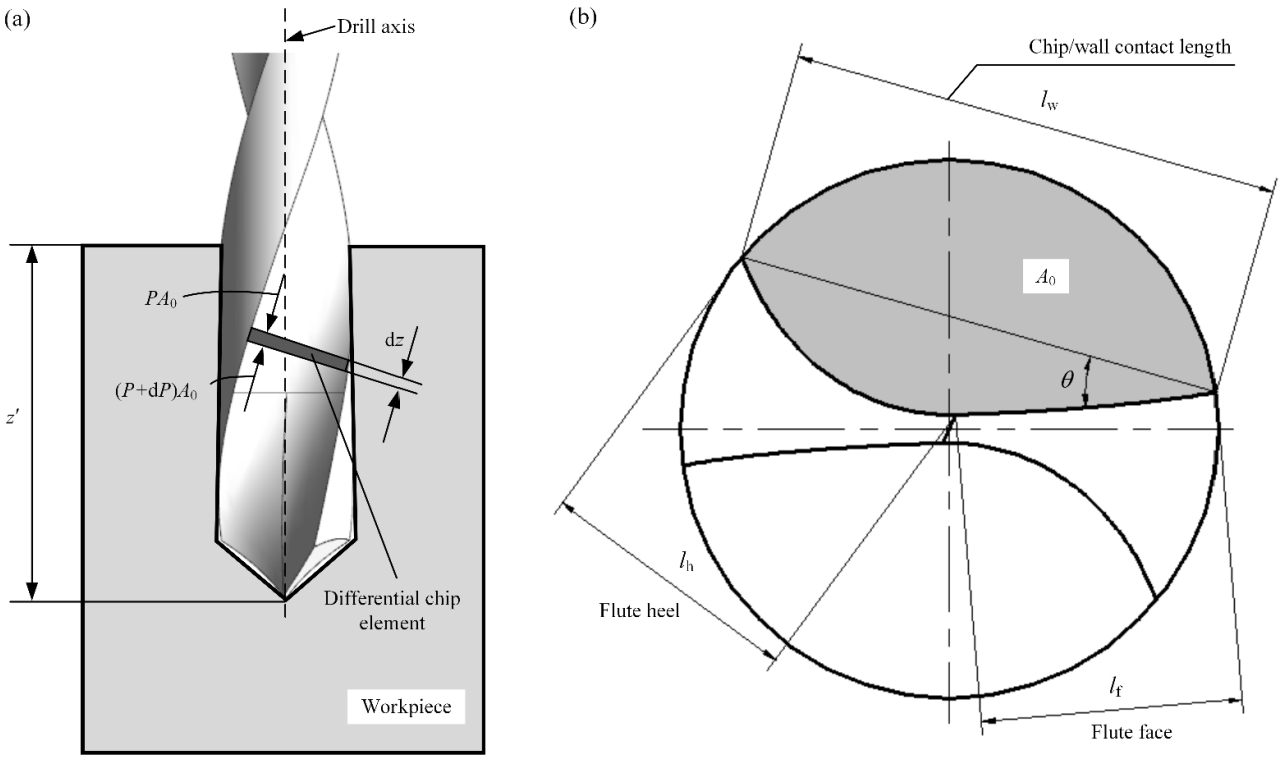

FIGURE 2. (a) Force balance of the differential chip element along the drill flute, (b) flute cross section of the twist drill.

logarithmic polynomial model were selected to relate the cutting condition to the parameters, κ and ξ, respectively. The parameter models were developed as follows:

$$\kappa = \alpha_0 + \alpha_1 n + \alpha_2 f + \alpha_3 nf, \tag{8}$$

$$\xi = \beta_0 + \beta_1 \ln n + \beta_2 \ln f + \beta_3 \ln n \ln f. \tag{9}$$

Each calibration experiment was repeated three times to achieve reliability in measuring the axial force. These associated coefficients in (8) and (9) can be determined by performing regression analysis through the calibration experiments.

B. CHIP-CLOGGING PREDICTION

Peck drilling is widely used in deep-hole drilling to remove the chips from the flutes. A rapid increase in the force begins at the critical depth, which is defined as the onset of chip clogging. Therefore, the gradient of the chip-evacuation force can be utilized as the criterion to determine the critical depth. Evidently, the gradient of the chip-evacuation force can be obtained by differentiating (5) as:

$$\mathrm{d}F_z/\mathrm{d}z = \kappa\xi \mathrm{e}^{\xi z}. \tag{10}$$

Thus, the critical depth z^* can be calculated from (10) as:

$$z^* = 1/\xi \left[\ln\left(1/\kappa\xi\right) + \ln\left(\mathrm{d}F_z^*/\mathrm{d}z\right)\right]. \tag{11}$$

The value of $\mathrm{d}F_z^*/\mathrm{d}z$ could be obtained by analyzing the experimental data from the calibration experiments. The modeling procedure of $\mathrm{d}F_z^*/\mathrm{d}z$ is demonstrated in the flow chart, as shown in Figure 4. First, the depth where the chip-evacuation force abruptly increased was identified as the critical depth. Secondly, the value of $\mathrm{d}F_z^*/\mathrm{d}z$ for each calibration experiment was calculated by substituting the critical depth into (10). Finally, the model of $\mathrm{d}F_z^*/\mathrm{d}z$ was established as a function of the spindle speed and the feed, as shown in (12), and the relevant coefficients were determined through the calibration experiments.

$$\mathrm{d}F_z^*/\mathrm{d}z = \lambda_0 + \lambda_1 \ln n + \lambda_2 \ln f + \lambda_3 \ln n \ln f \tag{12}$$

Notably, the chip-evacuation force model should be validated before the gradient model of the chip-evacuation force was established.

C. DRILLING EXPERIMENTS

1) BONE SPECIMEN

Drilling tests were conducted on fresh bovine tibia to calibrate the model parameters and assess the effectiveness of the developed model. Two tibiae were obtained from a nearby butcher's shop with no prior disease or fracture, and the average age of the cattle was 1.5 years. Each tibia was sectioned into four 50 mm blocks from the mid-diaphysis along the longitudinal direction of the tibia, and thereafter, the soft tissues and marrow were removed. All the specimens were maintained in physiological saline at a temperature of 3 °C for keeping the bones fresh prior to experiments and thawed to room temperature before the actual cutting.

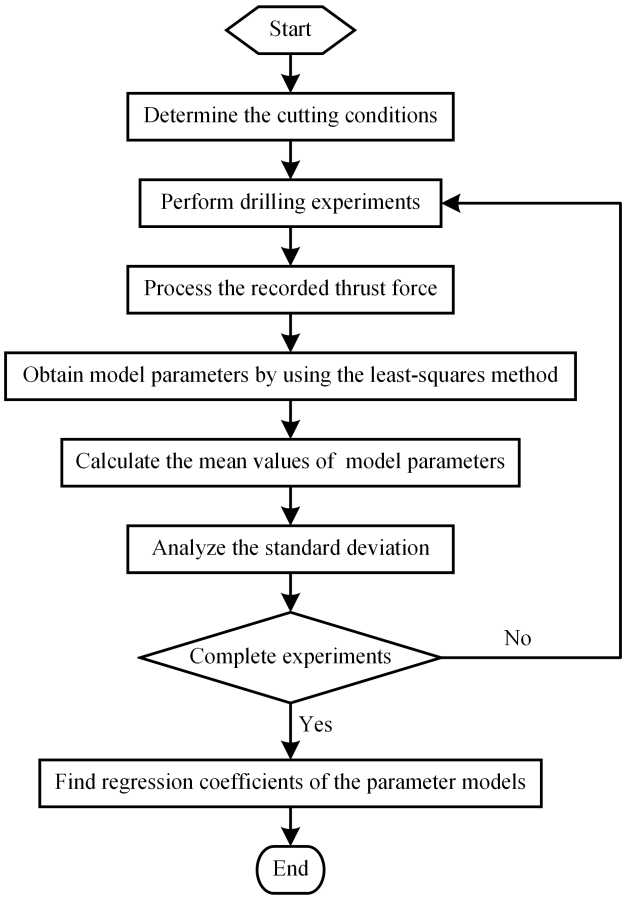

FIGURE 3. Flow chart of calibration procedure for the force model.

2) MEASUREMENT EQUIPMENT

Drilling experiments were conducted by using a vertical machining center (DAEWOO ACE-500) with a maximum spindle speed of 10000 r/min. The 2-mm-diameter twist drill with a helix angle of 25° and a point angle of 120° was used for all the tests. The drilling process was carried out through the clockwise rotation and down feeding of the spindle. The thrust force and torque generated during the drilling process were measured via a three-component dynamometer (Kistler type 9257B, Switzerland). The dynamometer was fixed on the smooth surface of the workbench of the machine before drilling. The workpiece was clamped by using the clamping device, which contains a U-plate, two symmetrical splints, and two screws, as shown in Figure 5. The U-plate was mounted on the dynamometer with four socket-headed cap screws. The drilling position can be changed by using the screws for different holes. A multichannel charge amplifier (Kistler amplifier 5070) was used to amplify the electrical signals from the transducers. The amplified signals were captured via a data acquisition card and were exported to a personal computer for further analysis.

3) DRILLING PARAMETER

The drilling tests were performed at room temperature under dry conditions. During the drilling processes, the computer simultaneously recorded and stored the thrust force obtained from the transducer. The drilling parameters used in the calibration and validation experiments are listed in Tables 1 and 2, respectively. According to the actual clinical applications, rotating speeds in the range 600 r/min to 1400 r/min were used, and the feeds were chosen in the range of 0.0071–0.0833 mm/r. Each set of drilling parameter listed in Table 1 was repeated three times to achieve reliability in measuring the thrust force. The average values of κ, ξ, and dF_z^*/dz were calculated for each calibration test. Four holes were produced in each specimen, resulting in 32 sets of force–depth curves. The same drilling depth (10 mm) was adopted in all the tests.

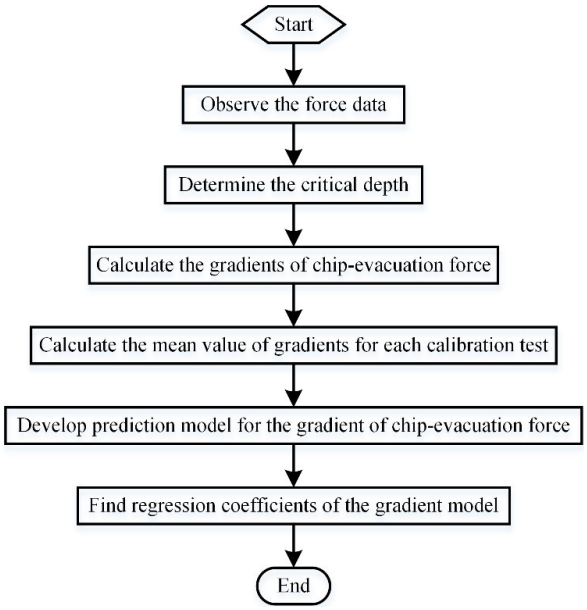

FIGURE 4. Procedure of gradient modeling.

TABLE 1. List of operating parameters for calibration experiments.

Calibration test No.	Spindle speed n (r/min)	Feed f (mm/r)
C1	600	0.0167
C2	600	0.0833
C3	1000	0.0200
C4	1000	0.0400
C5	1200	0.0167
C6	1200	0.0417
C7	1400	0.0071
C8	1400	0.0357

III. RESULTS

A. CHIP-EVACUATION FORCE MODEL

1) PARAMETERS OF FORCE MODEL

The typical plot of the thrust force varying with the depth was obtained after the cutting force was processed, as shown in Figure 6. A rapid increase in the thrust force can be seen

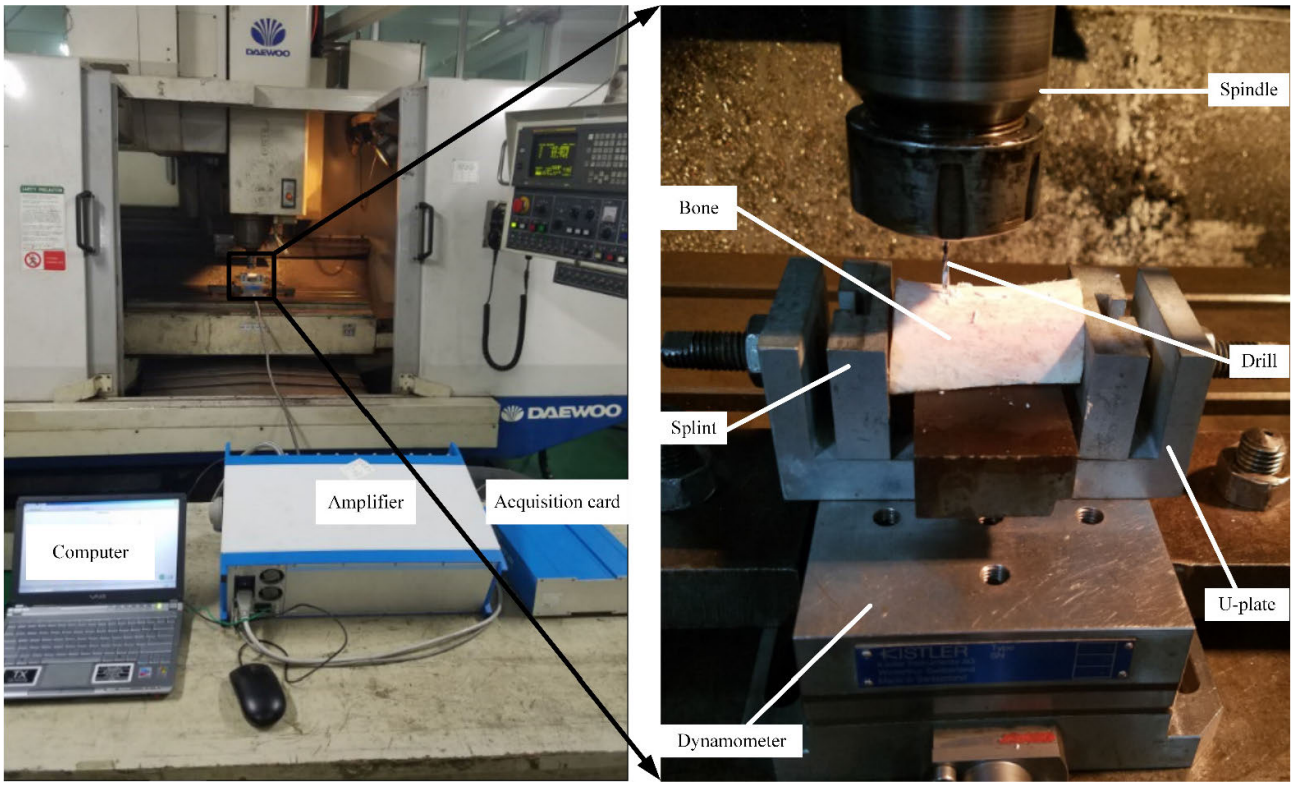

FIGURE 5. Schematic of drilling experiment.

TABLE 2. Cutting parameters used in validation experiments.

Validation test No.	Spindle speed n (r/min)	Feed f (mm/r)
V1	600	0.0333
V2	600	0.0500
V3	800	0.0125
V4	800	0.0375
V5	1000	0.0300
V6	1200	0.0083
V7	1200	0.0250
V8	1400	0.0286

after the critical depth. According to the discrete data from the experiments, the fitting curves were drawn by using the least-squares method. Then, the parameters, κ and ξ could be gained for each calibration test, as shown in Table 3.

The calculated standard deviation (SD) for each parameter indicates the concentrated data obtained from the calibration tests. Table 3 shows that the interactive effect of the spindle speed and feed on the parameter κ was significant. A similar situation of the coefficient ξ was observed for the selected cutting conditions. The value of κ varied for all the calibration experiments, with test C2 having the highest value and test C7 having the lowest. The average value of ξ in test C8 was 54% higher than that in test C2. The data demonstrated that the spindle speed and the feed played important roles in terms of the obtained parameters.

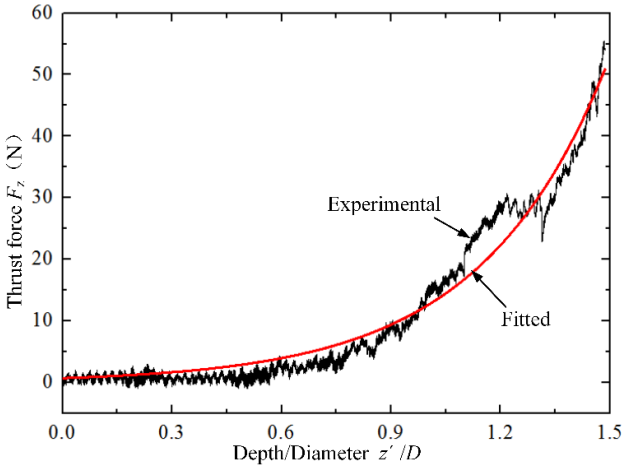

FIGURE 6. Experimental and fitted chip-evacuation force for calibration test C2.

2) ASSOCIATED REGRESSION COEFFICIENTS OF PARAMETER MODELS

According to the values of parameter κ in Table 3, a polynomial regression procedure was conducted to find the associated regression coefficients of the κ model given in (8). The regression coefficients of the ξ model given in (9) were determined in the same manner as the κ model. The results are shown in Table 4. The analysis of variance (ANOVA) was followed for the regression models to explore the significance of the effect of the cutting condition (the spindle speed and the

TABLE 3. Fitting results for calibration experiments.

Calibration test No.	κ				ξ			
	Replicate			SD	Replicate			SD
	1	2	3		1	2	3	
C1	0.1320	0.1267	0.1158	0.0067	3.8857	3.7855	3.9273	0.0595
C2	0.7070	0.6924	0.6793	0.0113	2.8771	2.8275	2.9059	0.0324
C3	0.1403	0.1227	0.1138	0.0606	4.3295	3.9413	3.9551	0.1798
C4	0.2263	0.2316	0.2478	0.0091	4.1984	3.9839	4.2086	0.1036
C5	0.0841	0.0770	0.0784	0.0031	4.0473	4.3267	4.1582	0.1149
C6	0.1413	0.1377	0.1396	0.0015	4.0325	4.5473	4.1454	0.2209
C7	0.0242	0.0268	0.0254	0.0011	4.0824	3.9627	4.1242	0.0684
C8	0.0928	0.0951	0.1075	0.0065	4.4050	4.2442	4.6026	0.1466

TABLE 4. Coefficients for the mechanistic force and gradient models.

Item	0	1	2	3
α	-0.0238	3.1490e-5	13.1863	-0.0080
α'	11.7854	-1.5977	2.7264	-0.3713
β	-28.1586	4.6150	-7.1211	1.0172
λ	-192.1110	33.3355	-35.7431	5.8976

feed) on the parameters. At a 95% confidence, the results are shown in Table 5.

The meanings of the variance analysis results are as follows: i) the sum of squares reflects the degree of deviation from the mathematical expectation and ii) the F value, a critical indicator to test the significance of the model, is the ratio of the two mean squares, and its calculated value should be greater than the threshold obtained from the F table. The results demonstrated that the effects of the spindle speed and the feed on the parameters were significant. R^2, also known as the coefficient of determination (COD), is a statistical measure to qualify the regression. The CODs for models (8) and (9) were 0.995 and 0.991, respectively. Therefore, the proposed models can be used to reveal the relationship between the parameters of the force model and the cutting condition.

3) MODEL VALIDATION

Validation experiments were conducted under different cutting conditions (Table 2) to assess the availability of the chip-evacuation force model presented above. The first step of the validating procedure was to determine the experimental parameters of the force model by using the nonlinear least-squares method shown in (6). A goodness-of-fit analysis was performed to explore the fitting degree of the force model to the measured data. Afterwards, the predicted parameters

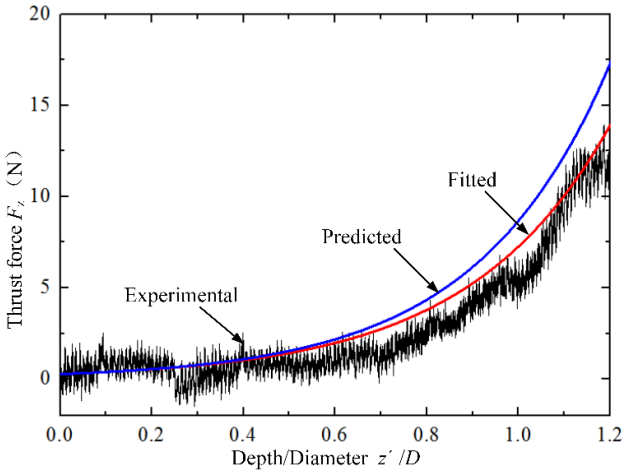

FIGURE 7. Comparison between experimental and predicted chip-evacuation force for validation test V1.

of the chip-evacuation force model were calculated (Table 6) from the parameter models. Finally, the parameter models were assessed by comparing the predicted and experimental parameters of the chip-evacuation force model.

The chip-evacuation force data were plotted to compare the experimental and predicted results, as shown in Figures 7 and 8. As Table 6 shows, the CODs suggest that model (5) explains approximately more than 89% of the variability in the chip-evacuation force. In addition, it is clear from Figures 7 and 8 that the fitted line is valid for bone drilling in capturing the increasing trend of the measured data from the transducer. The relative errors of the parameters reported in Table 6 can give an idea of the precision of the predicted values. Apparently, the magnitude of the relative error was lower than 10% for each validation test, which indicates that the modified model can be applied to predict the chip-evacuation force experienced during the drilling of bone.

TABLE 5. Summary of ANOVA for parameter models.

Model	Item	Sum of squares	DF	Mean square	F value	Prob > F
	Regression	0.602	4	0.1505	602	6.39
κ	Residual	0.001	4	0.00025		
	Total	0.603	8			
	Regression	128.249	4	32.06225	9160.5714	6.39
ξ	Residual	0.014	4	0.0035		
	Total	128.263	8			

TABLE 6. Results of experimental and predicted parameters for eight validation tests.

Validation test No.	R^2	Parameter κ			Parameter ξ		
		Experimental	Predicted	Relative error (%)	Experimental	Predicted	Relative error (%)
V1	0.9506	0.2813	0.2744	2.52	3.2509	3.4527	6.21
V2	0.8965	0.4204	0.4144	1.43	2.9484	3.2030	8.64
V3	0.9180	0.0953	0.0862	9.55	3.9554	4.0998	3.65
V4	0.8908	0.2431	0.2559	5.27	3.5222	3.7465	6.37
V5	0.9277	0.1489	0.1633	9.67	3.8275	4.0522	5.87
V6	0.9524	0.0472	0.0438	7.20	3.9526	4.1264	4.40
V7	0.9395	0.1055	0.1036	1.80	4.0447	4.2267	4.50
V8	0.9665	0.0740	0.0771	4.19	4.5028	4.3930	2.44

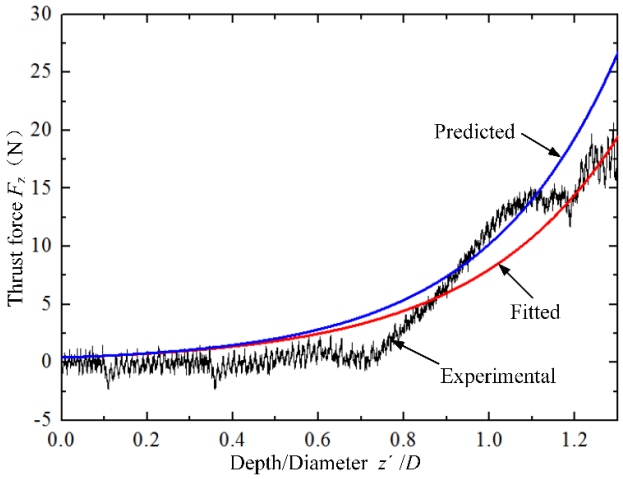

FIGURE 8. Comparison between experimental and predicted chip-evacuation force for validation test V2.

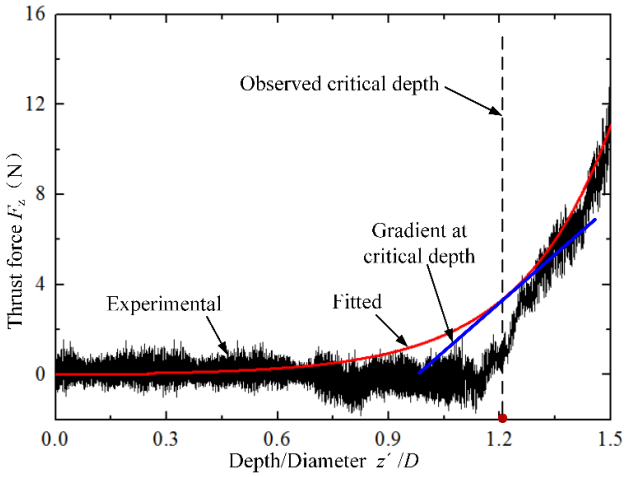

FIGURE 9. Observed critical depth for calibration test C7.

B. CHIP-CLOGGING PREDICTION

1) GRADIENT OF CHIP-EVACUATION FORCE

The selection for the gradient of the chip-evacuation force can be done by analyzing the experimental data from the calibration experiments. The point at which the chip-evacuation force begins to increase sharply was selected as the critical depth. As seen in Figures 9 and 10, the cutting condition plays an important role in terms of the observed critical depth. Therefore, it was essential to consider the spindle speed and the feed for chip-clogging prediction. Once this depth was chosen, the magnitude of dF_z^*/dz could be found by substituting the observed critical depth into (10) for each calibration test.

Table 7 presents the observed critical depths and the calculated gradients for eight calibration experiments. An interactive effect of the spindle speed and the feed was observed on the gradient. The calculated SD for the gradient varied from 1.19 to 2.90, which indicates that the concentrated data were obtained from the calibration tests. Thus, the average value in Table 7 can be taken as the experimental gradient for each calibration test.

TABLE 7. List of the observed critical depths and gradients for all the calibration tests.

Calibration test No.	Observed critical depth z^*			Gradient dF^*/dz at critical depth			
	Replicate			Replicate			Average
	1	2	3	1	2	3	
C1	0.8583	0.8432	0.8715	14.4031	11.6718	13.9392	13.3380
C2	0.7575	0.7028	0.7234	17.9836	14.2815	16.1542	16.1398
C3	0.8102	0.9016	0.9173	20.2720	16.8943	16.9405	18.0356
C4	0.7879	0.7780	0.7417	25.9645	20.4706	22.4509	22.9620
C5	0.9754	0.9481	0.9521	17.6377	20.1459	17.0845	18.2894
C6	0.8848	0.8297	0.9034	20.1958	27.2417	24.4830	23.9835
C7	1.2625	1.2365	1.1987	17.1040	14.2599	14.6955	15.3531
C8	0.9513	0.9656	0.8921	27.0019	24.3109	30.0342	27.1157

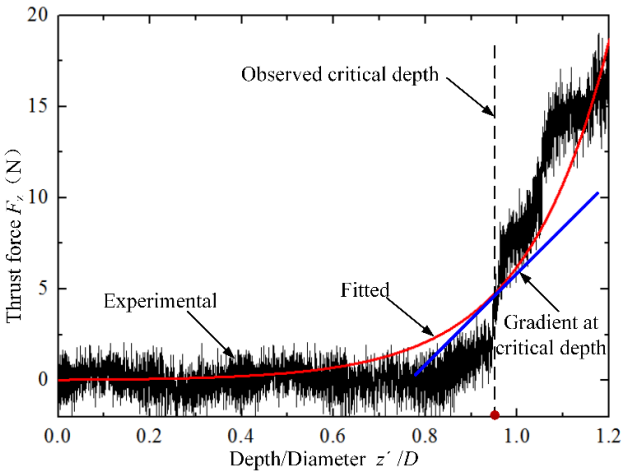

FIGURE 10. Observed critical depth for calibration test C8.

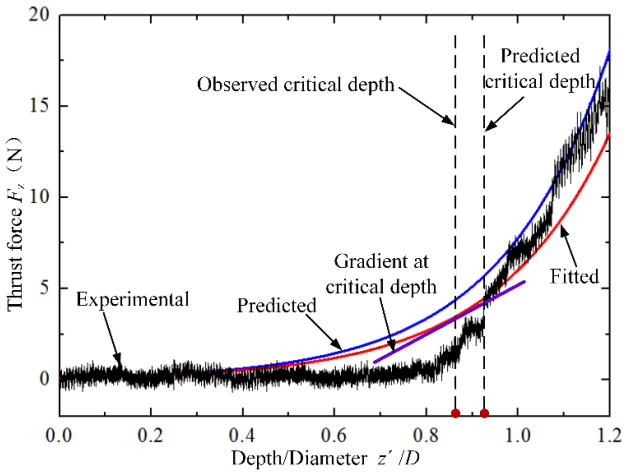

FIGURE 11. Experimental and predicted critical depths for validation test V7.

2) COEFFICIENTS OF GRADIENT MODEL

According to the experimental gradients presented in Table 7, the logarithmic polynomial regression given in (12) was utilized to develop the gradient model. The coefficients are presented in Table 4.

The ANOVA was followed for this regression model to explore the significance of the effect of the cutting condition (the spindle speed and the feed) on the gradient. At a 95% confidence, the variance analysis results given in Table 8 demonstrate that the cutting condition has a significant effect on the gradient of the chip-evacuation force. Moreover, the COD for the model was 0.971, which indicates that the regression line can account for almost all the variability of the tested data. Therefore, the correlation between the cutting condition and the gradient can be explained by using the proposed model given in (12).

3) MODEL VALIDATION

The critical depth where chip clogging occurs under different cutting conditions can be predicted by a combination of (8), (9), and (12). The validation tests were used to evaluate the precision of the chip-clogging prediction. The cutting conditions are shown in Table 2. The observed and predicted critical depths for two of the validation experiments are exhibited in Figures 11 and 12. In these figures, a close critical depth was found from the comparison between the experimental and predicted results.

The CODs in Table 6 suggest that models (8) and (9) can be used to predict the critical depth. Thus, the predicted critical depth was obtained by substituting (8), (9), and (12) into (11) with the coefficients given in Table 4, and it was compared to the experimental value for each validation experiment. The results are summarized in Table 9. It is clear that the magnitude of the relative error was lower than 10% for each validation test, which indicates that the modified force model can be applied to predict the formation of chip clogging during the drilling of bone.

IV. DISCUSSIONS

A. EFFECT OF CUTTING CONDITION ON PARAMETER κ

The values of κ obtained from the fitting curves for the calibration experiments were analyzed before calculating the

TABLE 8. Summary of ANOVA for gradient model.

Model	Item	Sum of squares	DF	Mean square	F value	Prob > F
	Regression	3166.982	4	791.746	682.540	6.39
dF^*/dz	Residual	4.639	4	1.160		
	Total	3171.621	8			

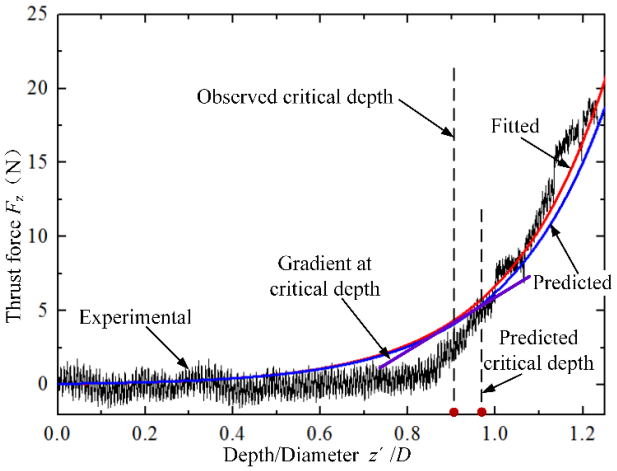

FIGURE 12. Experimental and predicted critical depths for validation test V8.

TABLE 9. Results of critical depth for eight validation experiments.

Validation test No.	Critical depth z^*		
	Experimental	Predicted	Relative error (%)
V1	0.7665	0.7879	2.79
V2	0.7543	0.7610	0.89
V3	0.9984	0.9076	9.09
V4	0.7592	0.7921	4.33
V5	0.8640	0.8490	1.74
V6	1.1306	1.0735	5.05
V7	0.8761	0.9249	5.57
V8	0.9047	0.9752	7.79

coefficients of the parameter model. Table 3 shows that the difference of κ between each level of the spindle speed varied with different levels of the feed. Therefore, the relationship between the parameter and the cutting condition cannot be established as a binary linear-regression equation, and the quadratic or other regression models should be considered. Thus, the logarithmic polynomial regression given in (13) and polynomial regression given in (8) were both analyzed for the modeling of κ. The regression coefficients for model (13) are given in Table 4. The CODs for models (13) and (8) were 0.998 and 0.995, respectively, which indicates that the logarithmic polynomial and polynomial regressions can well reflect the correlation between the parameter and the cutting condition. In addition, the COD of the logarithmic polynomial regression was slightly higher than that of the

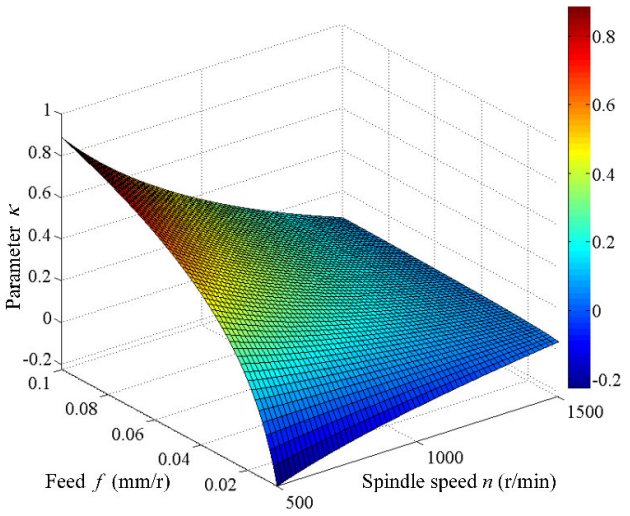

FIGURE 13. 3D surface for parameter κ obtained from the logarithmic polynomial regression.

polynomial regression.

$$\kappa = \alpha_0' + \alpha_1' \ln n + \alpha_2' \ln f + \alpha_3' \ln n \ln f \tag{13}$$

The three-dimensional (3D) surfaces were plotted by using (13) and (8) to compare the two developed models, as shown in Figures 13 and 14. These figures show that i) a similar variation trend of κ was found for the two models under the selected spindle speeds and feeds and ii) the value of κ obtained from the logarithmic polynomial regression was less than zero under certain cutting conditions, which differs from reality as the chip-evacuation force is greater than zero. Hence, the logarithmic polynomial regression model was unsuitable for predicting κ, and the polynomial regression was chosen in the current analysis.

To investigate the effect of cutting condition on the parameter κ, the 3D surface shown in Figure 14 indicates that the value of the parameter increased significantly when the feed increased from 0.0071 to 0.1 mm/r for the range of spindle speed used. The maximum value appeared at the position with the lowest spindle speed and the highest feed. When the feed varied in the range of 0.0071–0.06 mm/r, the value of κ varied in a small range. However, a significant decrease in the parameter was observed when the spindle speed increased from 500 to 1500 r/min with a feed in the range of 0.06–0.1 mm/r. The minimum value of κ appeared at the position with the largest spindle speed and smallest feed.

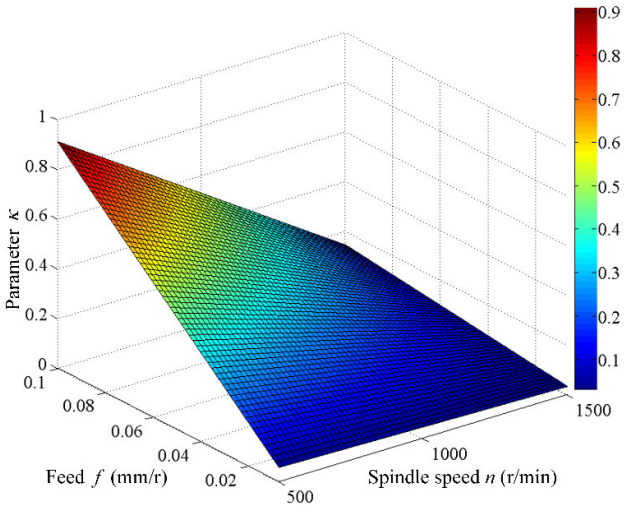

FIGURE 14. 3D surface for parameter κ obtained from the polynomial regression.

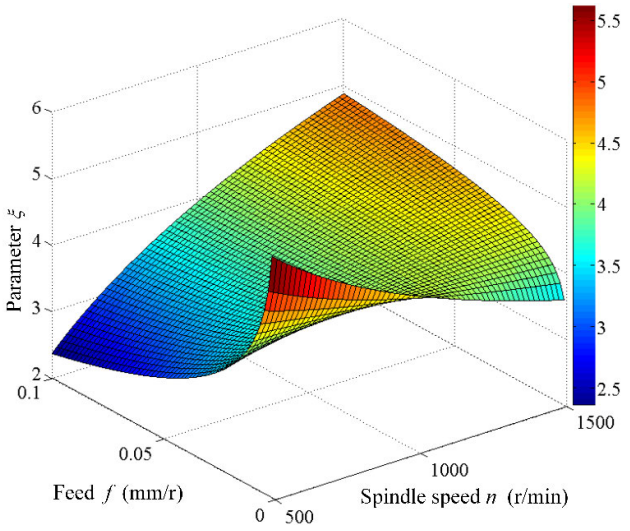

FIGURE 15. 3D surface for parameter ξ obtained from the logarithmic polynomial regression.

B. EFFECT OF CUTTING CONDITION ON PARAMETER ξ

Based on the parameter obtained from the calibration tests, data analysis was conducted to develop the prediction model of ξ. Similarly, the effect of the spindle speed and the feed on this parameter is interactive, and the prediction model cannot be simply expressed as a linear-regression equation. The parameter of the chip-evacuation force model, ξ, was considered as a function of spindle speed and feed using two common regression equations, the logarithmic polynomial and polynomial regressions. The CODs for the logarithmic polynomial and polynomial regressions were 0.991 and 0.989, respectively. Therefore, the logarithmic polynomial regression was chosen in this study because of its higher goodness of fit.

Figure 15 illustrates how the parameter changes with the selected cutting conditions for the logarithmic polynomial regression. From this figure, the following points can be obtained. i) The parameter ξ varied in a small range with a lower value when the spindle speed was less than 900 r/min with a feed in the range of 0.03–0.1 mm/r. ii) For the range of feed used, the value of ξ decreased significantly with the increase in the feed when the spindle speed varied in the range of 500–900 r/min. The minimum value of ξ appeared at the position with the lowest spindle speed and highest feed. iii) The effect of feed on the parameter was not remarkable when the rotational speed changed in the range 900 to 1200 r/min. iv) There was a significant increase in the parameter when the feed increased from 0.0071 to 0.1 mm/r with a spindle speed in the range of 1200–1500 r/min. Therefore, both spindle speed and feed played important roles in determining the chip-evacuation performance.

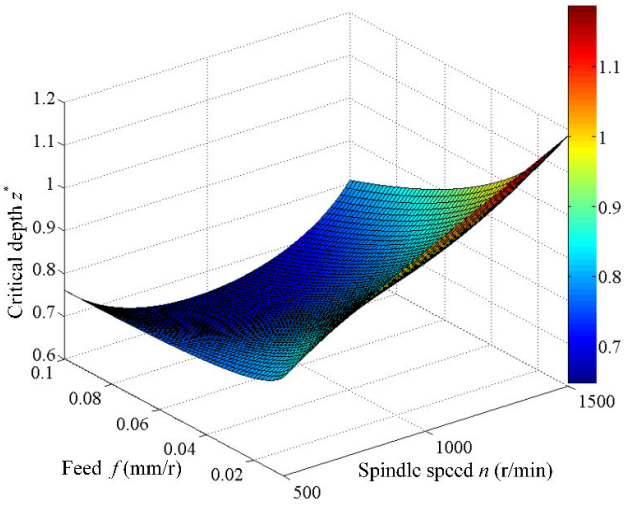

FIGURE 16. 3D surface for parameter critical depth $z*$.

C. EFFECT OF CUTTING CONDITION ON CRITICAL DEPTH

To develop the prediction model of chip clogging, the selection of dF_z^*/dz was made by analyzing the calibration data listed in Table 7. Previous study reported that a quadratic polynomial equation [30] can be considered as representative of the gradient performance while this equation was applied for drilling of metal. In the present work, two common regression models, i.e., the logarithmic polynomial and polynomial regressions were both analyzed to find the appropriate model for the gradient of the chip-evacuation force. The CODs were 0.971 and 0.967 for the logarithmic polynomial and polynomial regressions, respectively, which indicates that the logarithmic polynomial regression is more suitable for the gradient modeling.

Figure 16 provides a visualized view for the effect of the cutting condition on the critical depth. The figure reveals that the level of the critical depth was lower under the cutting conditions with a spindle speed in the range of 500–800 r/min and a feed in the range of 0.06–0.1 mm/r. This indicates that bone chips are prone to cluster on the flute surface and

block the removal of additional material under these cutting conditions, suggesting that these cutting conditions should be avoided in the drilling of cortical bone. Secondly, the critical depth decreased significantly with an increase in the feed when the spindle speed varied in the range of 800–1500 r/min. Moreover, a significant increase in the critical depth could be observed when the spindle speed changed from 500 to 1500 r/min with a feed in the range of 0.06–0.1 mm/r. The critical depth reached the maximum value with a spindle speed of 1500 r/min and a feed of 0.0071 mm/r, which suggests that a combination of low feed and high rotational speed may improve the quality of the hole and the productivity when step-by-step method is used in the drilling of cortical bone. Nevertheless, the temperature increases with an increase in the spindle speed [31]. Consequently, both the critical depth and temperature should be considered when determining the optimal values for the cutting parameters. It can be concluded that both spindle speed and feed played important roles in determining the critical depth.

D. FACTORS AFFECTING PREDICTION ACCURACY OF CHIP CLOGGING

To gain a better understanding of the results, the factors that affect the prediction accuracy of chip clogging must be investigated. The measurement error in the geometric parameters of the twist drill was eliminated because these geometric parameters were regarded as constants, as shown in (3). However, the measuring error would affect the prediction accuracy of previous models reported in the literature [27], [30] because the chip-evacuation force was modeled based on the flute geometry. Obviously, the effect of tool wear was ignored in the present study. Additionally, for the sake of simplicity, the coefficients of friction were assumed to be constants under the same cutting condition. The experimental critical depths for calibration tests were obtained by observing the discrete data, which would have an effect on the predicted results for chip clogging. Although somewhat subjective, this method was proved to be effective.

Cortical bone is highly hierarchical composite biomaterial [32] with different microstructures, such as osteons and interstitial lamellar bone. It has been shown in previous research that the intrinsic anisotropic nature of the cortical bone has a significant influence on the cutting force [33]. All experiments in the current study were conducted in the direction perpendicular to the long axis of the bone. The chip-evacuation force experienced during the drilling of cortical bone in different orientations should be examined because of the considerable effect of anisotropy. The effect of drying should receive attention, because cooling plays an important role in determining the level of chip-evacuation force. Moreover, the study of Pourkand *et al.* [34] suggests that the influence of bone density on the cutting force is considerable. These aspects will be considered in future work. Finally, other factors that influence the prediction accuracy are specimen pretreatment, fixation of the bone, air moisture content, etc.

V. CONCLUSION

A modified model for predicting the chip-evacuation force experienced during the drilling of cortical bone was developed by using a dental twist drill. The modified force model was then used to estimate the emergence of chip clogging. The main conclusions are presented below.

i) The chip-evacuation force model was established as a function of process parameters based on the elemental chip flow method. The two parameters related to the force model were determined through calibration tests under different cutting conditions. The parameter models were considered as functions of spindle speed and feed.

ii) A series of validation experiments was conducted to analyze the validity of the chip-evacuation force model. The relative errors of the two parameters were less than 10% for each validation test. The predicted results of the model parameters were demonstrated to be consistent with the experimental ones.

iii) The critical depth for chip clogging was predicted based on the slope of the chip-evacuation force. The gradient model was considered as a function of the spindle speed and the feed. It was proved that the modified chip-evacuation force model can be employed to predict the onset of chip clogging in the drilling of cortical bone.

iv) Both spindle speed and feed should be important considerations during bone drilling, because they had significant effects on the chip-evacuation force and chip clogging. Combinations of spindle speed in the range of 500–800 r/min and feed in the range of 0.06–0.1 mm/r should be avoided, because chip clogging was likely to emerge under these conditions.

ACKNOWLEDGMENT

The authors highly appreciate their colleagues at Shandong University for conduct of the experiments. Furthermore, the authors would like to thank the reviewers for their valuable comments and editors for improving the manuscript.

REFERENCES

[1] K. L. Wiggins and S. Malkin, "Drilling of bone," *J. Biomech.*, vol. 9, no. 9, pp. 553–559, 1976.

[2] Z. Liao and D. A. Axinte, "On monitoring chip formation, penetration depth and cutting malfunctions in bone micro-drilling via acoustic emission," *J. Mater. Process. Technol.*, vol. 229, pp. 82–93, Mar. 2016.

[3] R. J. Furness, A. G. Ulsoy, and C. L. Wu, "Supervisory control of drilling," *ASME J. Eng. Ind.*, vol. 118, no. 1, pp. 10–19, Feb. 1996.

[4] V. Bogovicč, A. Svete, K. Rupnik, and I. Bajsić, "Experimental analysis of the temperature rise during the simulation of an implant drilling process using experimental designs," *Measurement*, vol. 63, pp. 221–231, Mar. 2015.

[5] K. N. Bachus, M. T. Rondina, and D. T. Hutchinson, "The effects of drilling force on cortical temperatures and their duration: An *in vitro* study," *Med. Eng. Phys.*, vol. 22, no. 10, pp. 685–691, Dec. 2000.

[6] Y. Cai, X. Chen, J. Yu, and J. Zhou, "Numerical study on the evolution of mesoscopic properties and permeability in sandstone under hydromechanical coupling conditions involving industrial Internet of Things," *IEEE Access*, vol. 6, pp. 11804–11815, 2018.

[7] W. Wang and A. Elbanna, "Crack propagation in bone on the scale of mineralized collagen fibrils: Role of polymers with sacrificial bonds and hidden length," *Bone*, vol. 68, pp. 20–31, Nov. 2014.

[8] X. Chen, "Positive modulation of osteogenesis on a titanium oxide surface incorporating strontium oxise: An *in vitro* and *in vivo* study," *Mater. Sci. Eng. C Mater. Biol. Appl.*, vol. 99, pp. 710–718, Jun. 2019.

[9] S. A. Gehrke, R. Bettach, J. S. A. Júnior, J. C. Prados-Frutos, M. D. Fabbro, and J. AwadShibli, "Peri-implant bone behavior after single drill versus multiple sequence for osteotomy drill," *Biomed Res. Int.*, vol. 2018, Apr. 2018, Art. no. 9756043.

[10] E. Bağci and B. Ozcelik, "Investigation of the effect of drilling conditions on the twist drill temperature during step-by-step and continuous dry drilling," *Mater. Des.*, vol. 27, no. 6, pp. 446–454, 2006.

[11] D. W. Kim, Y. S. Lee, M. S. Park, and C. N. Chu, "Tool life improvement by peck drilling and thrust force monitoring during deep-micro-hole drilling of steel," *Int. J. Mach. Tools Manuf.*, vol. 49, nos. 3–4, pp. 246–255, Mar. 2009.

[12] G. Augustin, T. Zigman, S. Davila, T. Udilljak, T. Staroveski, D. Brezak, and S. Babic,, "Cortical bone drilling and thermal osteonecrosis," *Clin. Biomech.*, vol. 27, no. 4, pp. 313–325, May 2012.

[13] S. Ravisubramanian and M. S. Shunmugam, "Investigations into peck drilling process for large aspect ratio microholes in aluminum 6061-T6," *Mater. Manuf. Process.*, vol. 33, no. 9, pp. 935–942, 2018.

[14] J. Soriano, A. Garay, P. Aristimuño, L. M. Iriarte, J. A. Eguren, and P. J. Arrazola, "Effects of rotational speed, feed rate and tool type on temperatures and cutting forces when drilling bovine cortical bone," *Mach. Sci. Technol.*, vol. 17, no. 4, pp. 611–636, 2013.

[15] J. Sui and N. Sugita, "Experimental study of thrust force and torque for drilling cortical bone," *Ann. Biomed. Eng.*, vol. 47, no. 3, pp. 802–812, Mar. 2019.

[16] K. Alam, R. Muhammad, A. Shamsuzzoha, A. AlYahmadi, and N. Ahmed, "Quantitative analysis of force and torque in bone drilling," *J. Eng. Res.*, vol. 14, no. 1, pp. 39–48, 2017.

[17] W. A. Lughmani, K. Bouazza-Marouf, and I. Ashcroft, "Drilling in cortical bone: A finite element model and experimental investigations," *J. Mech. Behav. Biomed. Mater.*, vol. 42, pp. 32–42, Feb. 2015.

[18] X. Li, W. Zhu, J. Wang, and Y. Deng, "Optimization of bone drilling process based on finite element analysis," *Appl. Therm. Eng.*, vol. 108, pp. 211–220, Sep. 2016.

[19] G. J. M. Tuijthof, C. Frühwirt, and C. Kment, "Influence of tool geometry on drilling performance of cortical and trabecular bone," *Med. Eng. Phys.*, vol. 35, no. 8, pp. 1165–1172, Aug. 2013.

[20] C. H. Jacobs, M. H. Pope, J. T. Berry, and F. T. Hoaglund, "A study of the bone machining process-orthogonal cutting," *J. Biomech.*, vol. 7, no. 2, pp. 131–136, Mar. 1974.

[21] S. Saha, S. Pal, and J. A. Albright, "Surgical drilling: Design and performance of an improved drill," *ASME J. Biomech. Eng.*, vol. 104, no. 3, pp. 245–252, Aug. 1982.

[22] C. H. Jacobs, J. T. Berry, M. H. Pope, and F. T. Hoaglund, "A study of the bone machining process-drilling," *J. Biomech.*, vol. 9, no. 5, pp. 343–349, 1976.

[23] B. Allotta, G. Giacalone, and L. Rinaldi, "A hand-held drilling tool for orthopedic surgery," *IEEE/ASME Trans. Mech.*, vol. 2, no. 4, pp. 218–229, Dec. 1997.

[24] M. D. Tsai, M. S. Hsieh, and C. H. Tsai, "Bone drilling haptic interaction for orthopedic surgical simulator," *Comput. Biol. Med.*, vol. 37, no. 12, pp. 1709–1718, Dec. 2007.

[25] J. S. Strenkowski, C. C. Hsie, and A. J. Shih, "An analytical finite element technique for predicting thrust force and torque in drilling," *Int. J. Mach. Tools Manuf.*, vol. 44, nos. 12–13, pp. 1413–1421, Oct. 2004.

[26] L. Qi, X. Wang, and M. Q. Meng, "3D finite element modeling and analysis of dynamic force in bone drilling for orthopedic surgery," *Int. J. Numer. Methods Biomed. Eng.*, vol. 30, no. 9, pp. 845–856, Sep. 2014.

[27] T. Macavelia, A. Ghasempoor, and F. J. Sharifi, "Force and torque modeling of drilling simulation for orthopaedic surgery," *Comput. Methods Biomech. Biomed. Eng.*, vol. 17, no. 12, pp. 1285–1294, 2014.

[28] Y. Lin, H. Chen, D. Yu, Y. Zhang, and W. Yuan, "A predictive bone drilling force model for haptic rendering with experimental validation using fresh cadaveric bone," *Int. J. Comput. Assist. Radiol. Surg.*, vol. 12, no. 1, pp. 91–98, Jan. 2017.

[29] P. Pandithevan, N. V. M. Pandy, and V. Prasannavenkadesan, "Investigation of bone drilling for secure implant fixation in human femurs: Taguchi optimization and predictive force models with experimental validation," *J. Mech. Med. Biol.*, vol. 18, no. 6, 2018, Art. no. 1850061.

[30] J. C. Mellinger, "Modeling chip-evacuation forces and prediction of chip clogging in drilling," *ASME J. Manuf. Sci. Eng.*, vol. 124, pp. 605–614, Aug. 2002.

[31] M. Marco, M. Rodríguez-Millán, C. Santiuste, E. Giner, and M. H. Miguélez, "A review on recent advances in numerical modelling of bone cutting," *J. Mech. Behav. Biomed. Mater.*, vol. 44, pp. 179–201, Apr. 2015.

[32] D. T. Reilly and A. H. Burstein, "The mechanical properties of cortical bone," *J. Bone Joint Surg.*, vol. 56, no. 5, pp. 1001–1022, Jul. 1974.

[33] C. Santiuste, "The influence of anisotropy in numerical modeling of orthogonal cutting of cortical bone," *Compos. Struct.*, vol. 116, pp. 423–431, Sep./Oct. 2014.

[34] A. Pourkand, N. Zamani, and D. Grow, "Mechanical model of orthopaedic drilling for augmented-haptics-based training," *Comput. Biol. Med.*, vol. 89, pp. 256–263, Oct. 2017.

AIRONG ZHANG received the M.S. degree in mechanical engineering from Shandong University, Jinan, China, in 2013, where she is currently pursuing the Ph.D. degree in mechanical engineering. Her current research interests include mechanical modeling, fundamental mechanism of drilling in bone, cutting parameter optimization for bone drilling, and optimum design of dental drills.

SONG ZHANG received the Ph.D. degree in mechanical engineering from Shandong University, Jinan, China, in 2004. As a Visiting Scholar, he studied in The University of Alabama, Tuscaloosa, USA, from 2007 to 2008. He is currently working as a Professor with the School of Mechanical Engineering, Shandong University, China. His research fields are fundamental mechanism of high-efficiency cutting and machined surface integrity, biomechanics, dynamic model and optimum design of surgical tools, and so on.

CUIRONG BIAN received the M.M. degree in prosthodontics from Shandong University, Jinan, China, in 2004. As a Visiting Scholar, she studied in Hokkaido University, Sapporo, Japan, in 1999. She is currently a Professor and a Chief Physician with the Qilu Hospital of Shandong University. Her research fields are fixed porcelain repair, reconstruction of maxillofacial bone defects, implant surgery and design, design and fabrication of denture, and so on.

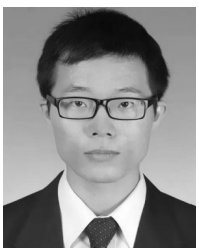

HUI KONG received the M.M. degree in prosthodontics from Shandong University, Jinan, China, in 2013. He is currently working as a Chief Physician with the Stomatology Department, Qilu Hospital of Shandong University. He is also a Senior Member of Plantation Association of Oral Hospital, Jinan, Shandong, China. His current research interests include complete denture restoration, aesthetic repair, and implant prosthesis.